Incorporation of Mean/Maximum Stress Effects in the Multiaxial Racetrack Filter

M.A. Meggiolaro[1], J.T.P. de Castro[1] and H. Wu[2]

[1] Pontifical Catholic University of Rio de Janeiro, PUC-Rio, Rua Marquês São Vicente, Rio de Janeiro, RJ, 22451-900, Brazil, meggi@puc-rio.br, jtcastro@puc-rio.br
[2] School of Aerospace Engineering and Applied Mechanics, Tongji University Siping Road 1239, 200092, Shanghai, P.R. China, wuhao@tongji.edu.cn

ABSTRACT. *In this work, the Multiaxial Racetrack Filter (MRF) is extended to incorporate mean or maximum stress effects, adopting a filter amplitude that depends on the current stress level along the stress or strain path. In this way, a small stress or strain amplitude event could be filtered out if associated with a non-damaging low-stress level, while another event with the very same amplitude could be preserved if happening under a more damaging high-stress level. The variable value of the filter amplitude must be calculated in real time, thus it cannot depend on peak or mean stresses along a load event, because it would require cycle identification and as so information about future events. Instead, mean/maximum stress effects are modeled in the filter as a function of the current (instantaneous) hydrostatic or normal stress along the load path, respectively for invariant-based and critical-plane models. The MRF efficiency is evaluated from tension-torsion experiments in 316L stainless steel tubular specimens under non-proportional (NP) load paths, showing it can robustly filter out non-damaging events even under multiaxial NP variable amplitude loading histories.*

INTRODUCTION

Unlike frequency filters that distort originally noisy signals, the uniaxial racetrack filter [1] is an efficient and well-proven technique to eliminate non-damaging events from uniaxial load histories without changing the original loading order and overall shape. Its generalization to multiaxial non-proportional (NP) variable amplitude loading (VAL) histories allows a dramatic reduction in computational cost while calculating fatigue damage from actual strain measurements, which are always noisy, oversampled, too long, and/or with too many non-damaging low-amplitude cycles.

However, the removal from multiaxial VAL histories of all data points that are not reversals of any of their stress or strain components is not appropriate because: (i) the path between two load reversals is needed to evaluate the path-equivalent stress or strain associated with each rainflow count, e.g. using a convex-enclosure method [2]; and (ii) reversal points from a multiaxial rainflow algorithm might not occur at the reversal of one of the stress or strain components.

A truly multiaxial racetrack filter (MRF) has been proposed in [3], performed on the load path represented in a sub-space from the 6D stress or strain space. The filter amplitude defines the radius of a hyper-sphere (or a sphere in 3D or a circle in 2D load histories, respectively), which translates along the load path while filtering out any small load oscillations happening within its interior region.

The use of a 5D deviatoric stress or strain space allows the MRF to be applied to invariant-based damage models, which assume fatigue damage is controlled by invariants like the von Mises ranges and hydrostatic stresses, such as Crossland's model [4]. For a given stress history, this 5D space is represented by the deviatoric vector

$$\vec{s}' \equiv \left[\sigma_x - (\sigma_y + \sigma_z)/2 \;\; (\sigma_y - \sigma_z)\sqrt{3}/2 \;\; \tau_{xy}\sqrt{3} \;\; \tau_{xz}\sqrt{3} \;\; \tau_{yz}\sqrt{3} \right]^T \tag{1}$$

Since the norm of $\vec{s}'$ is equal to the von Mises stress, all distances and filter amplitudes in this 5D sub-space have a physical meaning, they are the von Mises range or the relative von Mises stresses $\Delta\sigma_{Mises}$ for a straight path between two stress states. Alternatively, for a given strain history, the 5D space is defined by the deviatoric vector

$$\vec{e}' \equiv \left[\varepsilon_x - (\varepsilon_y + \varepsilon_z)/2 \;\; (\varepsilon_y - \varepsilon_z)\sqrt{3}/2 \;\; \gamma_{xy}\sqrt{3}/2 \;\; \gamma_{xz}\sqrt{3}/2 \;\; \gamma_{yz}\sqrt{3}/2 \right]^T \tag{2}$$

A sixth dimension could also be considered in the above 5D spaces, which would store the hydrostatic stress σ_h or strain ε_h of the current state, allowing the filtering of not only deviatoric components, but also of their hydrostatic components.

For 2D tension-torsion histories with stress paths defined by the normal and shear components σ_x and τ_{xy}, it is found that $\sigma_y = \sigma_z = \tau_{xz} = \tau_{yz} = 0$, while $\varepsilon_y = \varepsilon_z = -\bar{\nu} \cdot \varepsilon_x$ and $\gamma_{xz} = \gamma_{yz} = 0$, where $\bar{\nu}$ is an effective Poisson ratio. In this case,

$$\vec{s}' \equiv \left[\sigma_x \;\; 0 \;\; \tau_{xy}\sqrt{3} \;\; 0 \;\; 0 \right]^T \text{ and } \vec{e}' \equiv \left[\varepsilon_x \cdot (1+\bar{\nu}) \;\; 0 \;\; \gamma_{xy}\sqrt{3}/2 \;\; 0 \;\; 0 \right]^T \tag{3}$$

therefore the stress or strain paths of such tension-torsion histories can be represented in the 2D deviatoric diagrams $\sigma_x \times \tau_{xy}\sqrt{3}$ or $\varepsilon_x \cdot (1+\bar{\nu}) \times \gamma_{xy}\sqrt{3}/2$, which are sub-spaces from the 5D spaces from Eq. (3).

Figure 1 shows an idealized tension-torsion history represented in the $\sigma_x \times \tau_{xy}\sqrt{3}$ normal-effective shear stress diagram, with the original path points represented as × markers. For a (large) filter amplitude *r = 80MPa* (the radius of the circle shown in the figure), the MRF results in a much reduced number of points, represented with square and triangular markers. Note in the figure that many points from such oversampled example are filtered out. Note as well that small normal stress or effective shear stress oscillations are also filtered out, as seen in the upper part of the figure. The original *1,315* data points of this idealized history are dramatically reduced to only *56*, significantly reducing the computational cost of subsequent multiaxial rainflow or fatigue damage calculations.

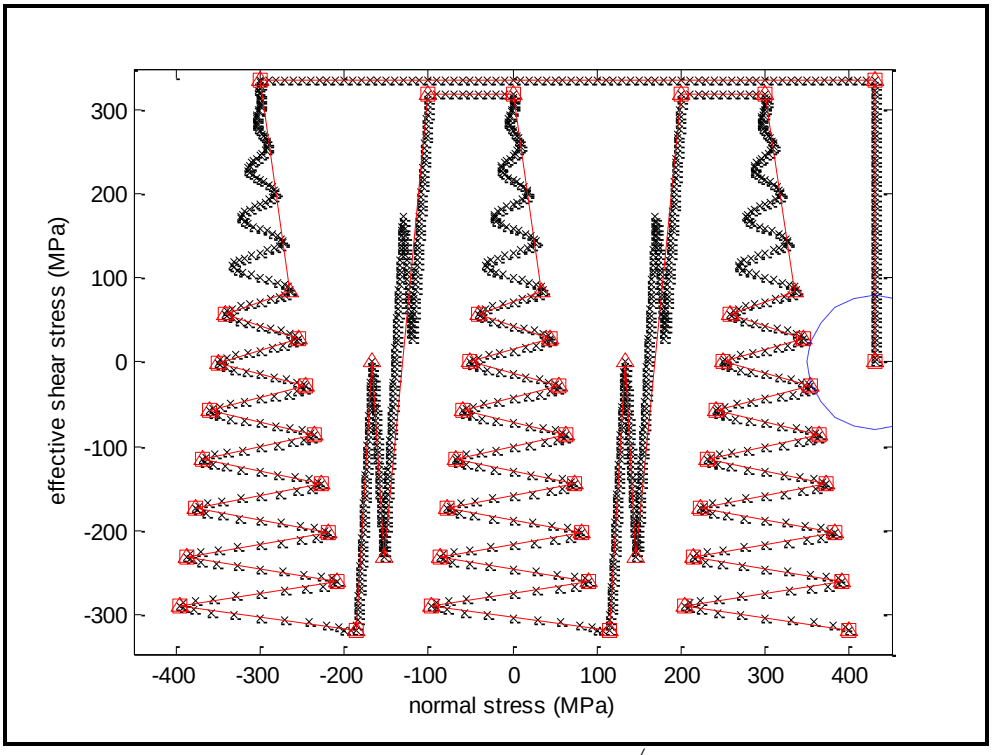

Figure 1. Original points from an idealized $\sigma_x \times \tau_{xy} \sqrt{3}$ stress path (× markers), and outputs from the MRF (square and triangular markers) for a filter amplitude $r = 80MPa$.

The MRF can also be applied to project histories on a candidate plane, useful to reduce computational cost in calculations from the critical-plane approach [5]. For shear-based damage models, the 2D spaces $[\tau_A \ \tau_B]^T$ or $[\gamma_A \ \gamma_B]^T$ could be adopted in the MRF, where the subscripts A and B represent the in-plane and out-of-plane shear directions of a candidate plane. For tensile-based damage models, the traditional uniaxial racetrack filter could be applied to the 1D spaces $[\sigma_\perp]$ or $[\varepsilon_\perp]$, where $\sigma_\perp$ and $\varepsilon_\perp$ are the normal stress and strain perpendicular to the considered candidate plane. Alternatively, for multiaxial models that mix both shear and tensile damage, the 3D stress or strain spaces $[\tau_A \ \tau_B \ \sigma_\perp]^T$ or $[\gamma_A \ \gamma_B \ \varepsilon_\perp]^T$ could be used instead in the MRF.

MRF WITH MEAN/MAXIMUM STRESS EFFECTS

The original implementation of the MRF [3] adopts a constant filter amplitude r. However, since tensile load histories tend to be more damaging due to mean/maximum stress effects in multiaxial fatigue, they would benefit from a choice of lower values of r, to avoid filtering out damaging events. On the other hand, compressive histories could allow the choice of higher filter amplitudes, filtering out more points without compromising the damage calculations.

Such an improved MRF, optimized to consider mean/maximum stress effects, can be implemented adopting a filter amplitude r that depends on the current stress level. In

this way, a small stress or strain amplitude event could be filtered out if associated with a non-damaging low-stress level, while another event with the same amplitude could be preserved if happening under a damaging high-stress level.

However, this is easier said than done. The filter amplitude must be calculated in real time (or else it would lose efficiency), therefore it cannot be a function of the peak or mean stresses along a load event, which would require cycle identification and information about future events. Instead, mean/maximum-stress effects are modeled in the filter in a simplified way, as a function of the current (instantaneous) hydrostatic σ_h or normal $\sigma_\perp$ stress along the load path, respectively for invariant-based and critical-plane models, as briefly outlined in [6].

Crossland's invariant-based model [4], e.g., adopts an infinite-life criterion

$$\Delta\tau_{Mises}/2+\alpha_C\cdot(3\cdot\sigma_{hmax})=\beta_C \tag{4}$$

where $\Delta\tau_{Mises}$ is a path-equivalent von Mises shear stress range, σ_{hmax} is the peak hydrostatic component, and α_C and β_C are material constants. If this damage model is adopted, then the stress history could be represented in the previously defined 5D deviatoric space $\vec{s}'$, assuming a σ_h-dependent variable filter amplitude

$$r\equiv\Delta\sigma_{Mises}/2=\Delta\tau_{Mises}\sqrt{3}/2=(\beta_C\sqrt{3})-(3\sqrt{3}\alpha_C)\cdot\sigma_h \tag{5}$$

On the other hand, Findley's critical-plane model [7] assumes that

$$\Delta\tau/2+\alpha_F\cdot\sigma_{\perp max}=\beta_F \tag{6}$$

where $\Delta\tau$ and $\sigma_{\perp max}$ are the shear stress range and peak normal stress on the critical plane, and α_F and β_F are material constants. Using this damage model, the shear stress history on the considered candidate plane could be represented in the 2D shear stress space $[\tau_A\ \tau_B]^T$, while adopting a $\sigma_\perp$-dependent variable filter amplitude

$$r\equiv\Delta\tau/2=\beta_F-\alpha_F\cdot\sigma_{\perp max} \tag{7}$$

Fatemi-Socie's critical-plane model [8] assumes that

$$\frac{\Delta\gamma}{2}\cdot\left(1+\alpha_{FS}\frac{\sigma_{\perp max}}{S_{Yc}}\right)=\frac{\tau_c}{G}(2N)^{b_\gamma}+\gamma_c(2N)^{c_\gamma} \tag{8}$$

where $\Delta\gamma$ and $\sigma_{\perp max}$ are the shear strain range and peak normal stress on the critical plane, N is the associated fatigue life in cycles, G and S_{Yc} are the material's shear modulus and cyclic yield strength, and α_{FS}, τ_c, γ_c, b_γ and c_γ are material constants. For this damage model, the shear strain history on the considered candidate plane could be represented in the 2D shear strain space $[\gamma_A\ \gamma_B]^T$, while adopting a $\sigma_\perp$-dependent variable filter amplitude

$$r \equiv \frac{\Delta\gamma}{2} = \left(\frac{\tau_c}{G} (2N_L)^{b_\gamma} + \gamma_c (2N_L)^{c_\gamma} \right) \Big/ \left(1 + \alpha_{FS} \frac{\sigma_\perp}{S_{Yc}} \right) \quad (9)$$

where N_L is the number of cycles associated with the stress-life fatigue limit, or any other user-defined fatigue life level.

A high-cycle variation of the above variable filter amplitude can also be defined, based on a shear stress instead of shear strain amplitude, giving

$$r = \tau_L / (1 + \alpha_U \cdot \sigma_\perp / S_U) \quad (10)$$

where τ_L is the shear fatigue limit under zero mean stresses, α_U is a material constant and S_U is its ultimate strength.

In all above cases for Crossland's, Findley's and Fatemi-Socie's models or its variations, the filter amplitude r becomes instantaneously smaller for higher σ_h or $\sigma_\perp$ stress levels, to avoid filtering out damaging events. Analogously, similar expressions for such a variable r could be easily derived for other multiaxial fatigue damage models.

RESULTS

The improved version of the MRF presented in this work is evaluated using experimental and idealized tension-torsion 2D stress histories. The experiments are performed on annealed tubular 316L stainless steel specimens in a multiaxial servo-hydraulic testing machine. The cyclic properties of this 316L steel are obtained from simple uniaxial tests. Its Ramberg-Osgood uniaxial cyclic hardening coefficient and exponent are 874MPa and 0.123, with Young's modulus 193GPa and Poisson ratio 0.3. But note that this material presents a significant non-proportional (NP) hardening effect as well, which cannot be neglected in multaxial fatigue damage calculations, as discussed below.

The experiments consist of strain-controlled tension-torsion cycles applied to two tubular specimens, one for the cross and one for the x-shaped paths from Fig. 2, represented in the normal-effective shear strain space $\varepsilon_x \times \gamma_{xy}/\sqrt{3}$. For each specimen, several load periods are applied for a given normal strain amplitude ε_a, for chosen strain amplitudes $\varepsilon_a = 0.2\%, 0.4\%, 0.6\%$ and 0.8%. The resulting normal-effective shear stress paths $\sigma_x \times \tau_{xy}\sqrt{3}$ are very complex, involving high NP hardening effects and transients, see Fig. 3.

Figure 3 shows the experimentally measured data points ($\times$ markers) from each of the two specimens, as well as the MRF output (solid lines) for a filter amplitude $r = 7MPa$. For the cross-shaped path, 95% of the measured points were filtered out, while for the x-shaped case 87% were eliminated, significantly reducing the computational costs of subsequent fatigue life calculations. Notice that, despite being highly filtered, the MRF outputs can almost exactly describe the original history, capturing not only all reversal points but also the path shape, which is a most important feature for equivalent-range calculations.

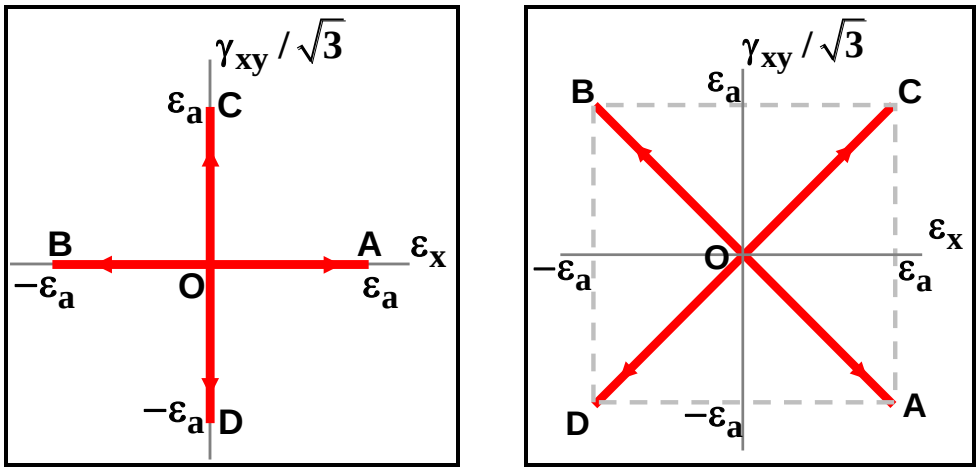

Figure 2. Applied $\varepsilon_x \times \gamma_{xy}/\sqrt{3}$ strain paths on two tension-torsion tubular specimens, with successively imposed amplitudes ε_a = *0.2%*, *0.4%*, *0.6%* and *0.8%* in each case.

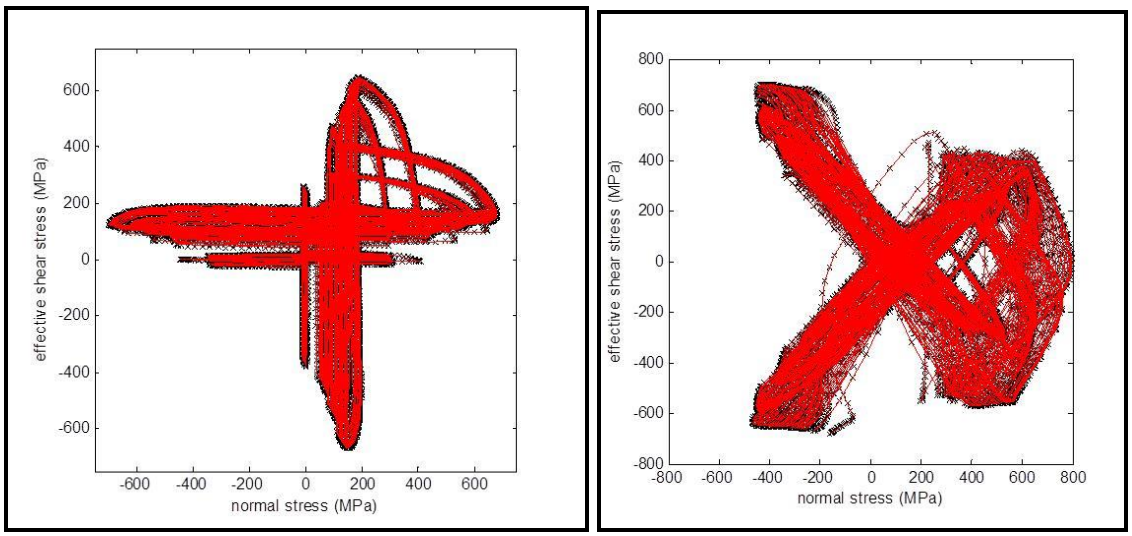

Figure 3. Experimentally measured data points (× markers) from the $\sigma_x \times \tau_{xy}\sqrt{3}$ stress paths induced by the cross and x-shaped inputs from Fig. 2, and associated outputs from the MRF (solid lines) for a chosen filter amplitude r = *7MPa*.

Figure 4 shows a random single period of each of the Fig. 3 paths, where the square markers represent the MRF output, filtering out most of the original stress points.

To better evaluate the mean/maximum stress effects in the proposed modification of the MRF, the idealized tension-torsion stress history from Fig. 1 is now filtered according to a filter amplitude based e.g. on Fatemi-Socie's model, shown in Eqs. (9) and (10) respectively for strain or stress histories. Figure 5 plots the idealized tension-torsion stress history in a normal-effective shear stress diagram, with the original path points represented as × markers.

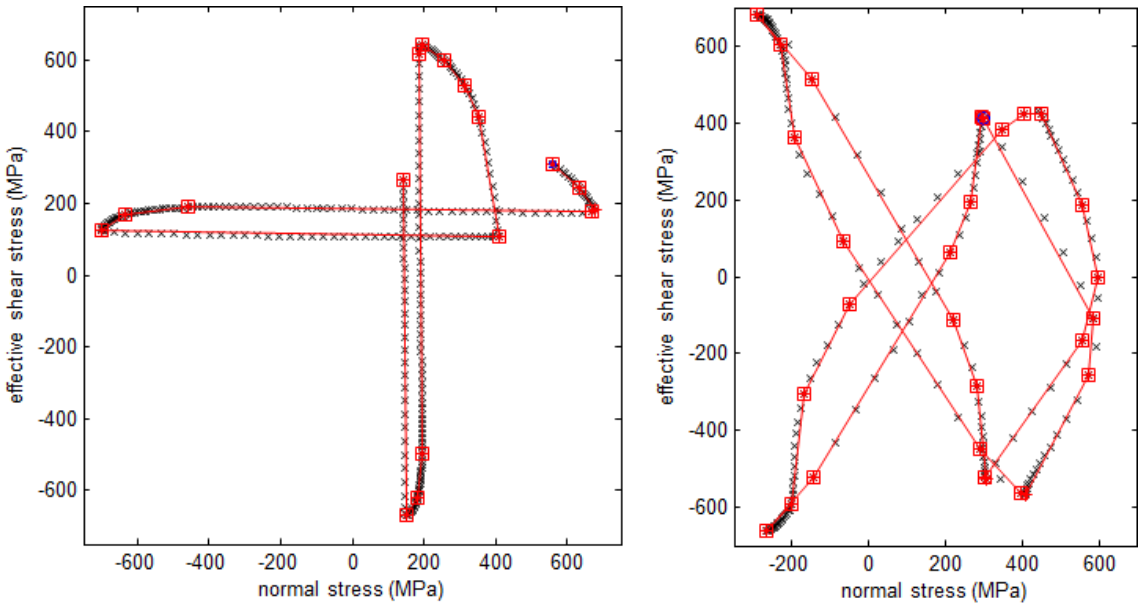

Figure 4. Experimentally measured data points (× markers) for a single period and associated outputs from the MRF (square markers) for a filter amplitude $r = 7MPa$.

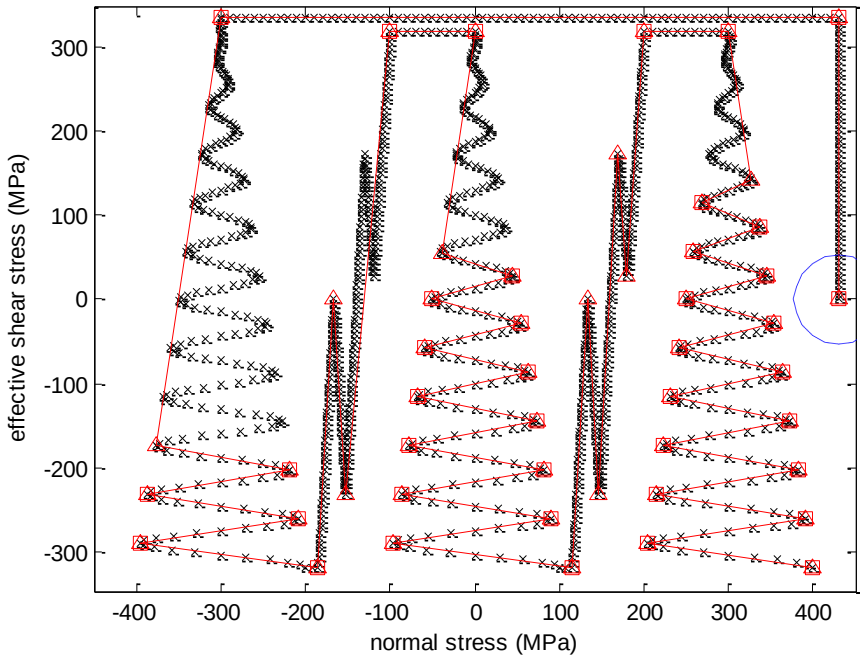

Figure 5. Original points from an idealized $\sigma_{\perp} \times \tau_A \sqrt{3}$ stress path (× markers), and outputs from the MRF (square and triangular markers), considering mean stress effects.

Assuming Fig. 5 represents the $\sigma_\perp \times \tau_A\sqrt{3}$ history of the normal stress and in-plane shear stress components on a candidate plane, the variable filter amplitude from Eq. (10) could be used, but multiplied by $\sqrt{3}$ (due to the scaling from τ_A to $\tau_A\sqrt{3}$) to give

$$r = \tau_L\sqrt{3}/\left(1+\alpha_U\cdot\sigma_\perp/S_U\right) \tag{11}$$

For a hypothetical component with $\tau_L\sqrt{3} = 80MPa$, S_U = *515MPa*, and α_U = *0.66*, the above variable filter amplitude becomes $r = 80/\left(1+0.66\cdot\sigma_\perp/515\right)$. Figure 5 shows the MRF output adopting such a variable *r*, where the remaining (unfiltered) points are marked as squares or triangles. Notice how most of the normal oscillations were filtered out under a –300MPa compressive mean normal stress, while very few of them were filtered under +300MPa. And the small shear cycle near the –120MPa compressive normal stress was filtered out, while the same shear cycle at +180MPa was not, a desirable behavior for an amplitude filter that considers mean/maximum stress effects.

CONCLUSIONS

The Multiaxial Racetrack Filter (MRF) is an efficient amplitude filter applicable to multiaxial histories and fatigue damage models based on invariant or on the critical-plane approach. The MRF is able to filter out low-amplitude events, significantly decreasing the computational cost of subsequent multiaxial fatigue-damage calculations. In this work, mean/maximum stress effects were incorporated into the MRF. The proposed variable filter amplitudes allowed the algorithm to efficiently filter out events based on their damage parameter. In this way, lower filter amplitudes are automatically used for tensile histories, and higher amplitudes for compressive ones, optimizing the filter efficiency without neglecting significant damaging events.

REFERENCES

1. Fuchs, H.O., Nelson, D.V., Burke, M.A., Toomay, T.L. (1973) SAE Automobile Engineering Meeting Paper 730565.
2. Meggiolaro, M.A., Castro, J.T.P. (2012) *Int J Fatigue* **42**, 217-226.
3. Meggiolaro, M.A., Castro, J.T.P., Wu, H. (2015) *Frattura ed Integrità Strutturale* **33**, 368-375.
4. Crossland, B. (1956) Int Conf Fatigue Metals, London: IMechE, 138-149.
5. Bannantine, J.A., Socie, D.F. (1991). In: *Fatigue under Biaxial and Multiaxial Loading v.10*, pp. 35-51, ESIS.
6. Wu, H., Meggiolaro, M.A., Castro, J.T.P. (2016) Validation of the multiaxial racetrack amplitude filter, International Journal of Fatigue **87**, 167–179.
7. Findley,W.N. (1959) *J Eng Industry* **81**, 301-306.
8. Fatemi, A, Socie, D.F. (1988) *Fatigue Fract Eng Mater Struct* **11**, 149-166.